

Closing the Door on the “Puzzle of Decoherence” of Annihilation Quanta

Siddharth Parashari^{a,*}, Damir Bosnar^a, Ivica Friščić^a, Zdenka Kuncic^b, Mihael Makek^{a,*}

^aDepartment of Physics, Faculty of Science, University of Zagreb, Bijenička c. 32, 10000 Zagreb, Croatia.

^bSchool of Physics, University of Sydney, Sydney, New South Wales, 2006, Australia

Abstract

In para-positronium annihilation, exploration of the polarization correlations of the emerging gamma quanta has gained interest, since it offers a possibility to improve signal-to-background in medical imaging using positron emission tomography. The annihilation quanta, which are predicted to be in an entangled state, have orthogonal polarizations and this property may be exploited to discriminate them from two uncorrelated gamma photons contributing to the background. Recent experimental studies of polarization correlations of the annihilation quanta after a prior Compton scattering of one of them, had rather different conclusions regarding the strength of the correlation after the scattering, showing its puzzling nature. The scattering was described as a decoherence process. In the present work, we perform for the first time, a study of the polarization correlations of annihilation quanta after decoherence via Compton scattering in the angular range $0^\circ - 50^\circ$ using single-layer gamma ray polarimeters. In addition, we compare the measured polarization correlations after Compton scattering at 30° with an active and a passive scatterer element. The results indicate that the correlation, expressed in terms of the polarimetric modulation factor, shows no significant difference at small scattering angles ($0^\circ - 30^\circ$) compared to the correlation measured for direct photons, while lower modulation was observed for 50° scattering angle.

Keywords: Para-Positronium annihilation ; Quantum entanglement ; Decoherence ; Gamma Polarization ; Positron Emission Tomography

*Corresponding authors

Email addresses: siddharth@phy.hr(Siddharth Parashari), makek@phy.hr (Mihael Makek)

1 Introduction

The correlation of gamma photons emerging from an annihilating positronium system has recently become an increasingly interesting research topic with a potential to bring substantial innovations to medical imaging with Positron Emission Tomography (PET) [1, 2, 3, 4, 5]. In para-positronium annihilation, two back-to-back γ quanta of 511 keV are produced with orthogonal polarizations and are predicted to be in an entangled state. This state can be described by the so called Bell state wave function $|\psi\rangle = (|X\rangle_- |Y\rangle_+ - |Y\rangle_- |X\rangle_+)/\sqrt{2}$, where, $|X\rangle_{+,-}$ and $|Y\rangle_{+,-}$ represent a quantum polarized in (X,Y) propagating in (+,-) \hat{z} direction [6, 7, 8, 9]. The measurement of correlations of annihilation quanta has a long history in physics, starting from the experimental scheme proposed by J. Wheeler [10] to test the predicted correlation of the polarizations of the annihilation photons, where the azimuthal angle difference ($\Delta\phi$) between the scattering planes in double Compton scattering process should have maxima and minima at 90° and 0° , respectively. Similar behavior is also predicted by Pryce and Ward [11] and Snyder *et al.* [8] by employing the Klein-Nishina approach [12], where the cross-section of a double Compton scattering process is given by [9, 11],

$$\frac{d^2\sigma}{d\Omega_1 d\Omega_2} = \frac{r_0^4}{16} [F(\theta_1)F(\theta_2) - G(\theta_1)G(\theta_2)\cos(2\Delta\phi)] \quad (1)$$

with r_0 being the classical electron radius, $d\Omega_{1,2}$ are the solid angles, $\theta_{1,2}$ are the Compton scattering angles, $\Delta\phi = (\phi_1 - \phi_2)$ is the azimuthal scattering angle difference of gamma particle 1 and 2, respectively. $F(\theta_{1,2}) = \frac{2+(1-\cos\theta_{1,2})^3}{(2-\cos\theta_{1,2})^3}$ and $G(\theta_{1,2}) = \frac{\sin^2\theta_{1,2}}{(2-\cos\theta_{1,2})^2}$ are kinematic factors. The ratio,

$$A(\theta) = \frac{N(\theta, \phi=90^\circ) - N(\theta, \phi=0^\circ)}{N(\theta, \phi=90^\circ) + N(\theta, \phi=0^\circ)} \quad (2)$$

defines the analyzing power of the polarimeter [13], where $N(\theta, \phi)$ is the number of incoming photons measured at scattering angle θ and azimuthal angle ϕ . The product of the analyzing powers $A(\theta_1)$ and $A(\theta_2)$ is known as the modulation factor (μ) and it measures the polarimetric sensitivity of the detection system. Bohm and Aharonov [6] recognized the azimuthal angle correlation in the double Compton scattering of annihilation photons could be considered an example of entanglement discussed by Einstein, Podolsky, and Rosen [14, 15]. Initially, it was shown theoretically that the ratio, $R = (1+\mu)/(1-\mu)$ of the scattering probabilities at $\Delta\phi=90^\circ$ and $\Delta\phi=0^\circ$, for the wave function in the predicted entangled (separable) state is $R \approx 2.8$ (1.63) [6, 8, 9, 11]. However, the question of evidence of entanglement in Compton scattering of annihilation quanta has been recently readdressed by theoretical works [16, 17] and it remains an open topic. The early experiments measured the modulation factors [18, 19, 20, 21, 22, 23, 24, 25], among which the most precise measurements were performed by Langhoff [19] and Kasday *et al.* [22], obtaining $R = 2.47 \pm 0.07$ and $R = 2.33 \pm 0.10$, respectively, which were in good agreement with the predicted value (eq. 1) considering the finite geometry of the detectors.

Recently, Watts *et al.* [4] used a simple polarimetric setup based on two Cadmium Zinc Telluride matrices to measure the azimuthal angle correlations of annihilation quanta directly from the source and in another configuration with a passive scatterer. In the latter, a Compton scattering may occur in the path of the photon prior to its detection in the polarimeter. In the measurement of the quanta direct from the source, they obtained a clear modulation of the azimuthal distribution with the measured $R = 1.95 \pm 0.07$ for $\theta_{1,2} = 93^\circ - 103^\circ$. In the configuration with the scatterer positioned at 33° relative to the initial direction, the results indicated the lack of modulation, within the experiment's precision, which they described as a "decohering" process.

In another experiment, Abdurashitov *et al.* [26] used a setup of two gamma-ray polarimeters, each

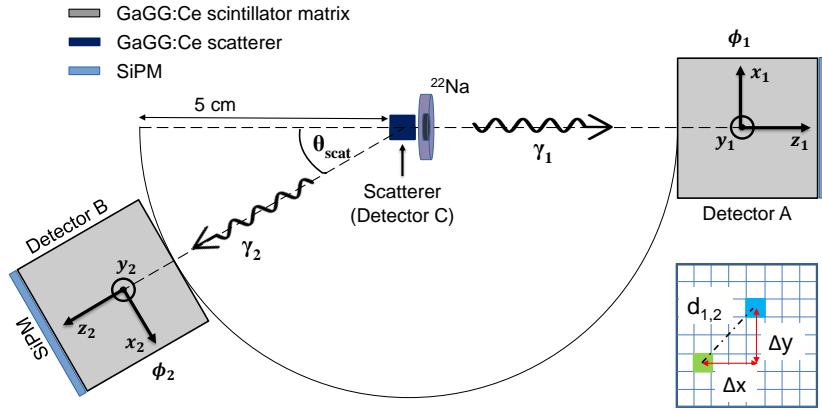


Figure 1: Schematic diagram of the experimental setup (top view). The azimuthal angles $\phi_{1,2}$ (eq. 3) and the inter-pixel distances $d_{1,2}$ are deduced from the relative positions of the fired pixels in the respective module.

consisting of 16 NaI(Tl) scintillator detectors positioned on a ring, with a plastic scatterer placed at the center. Such geometry enabled precise measurement of the azimuthal angle correlations in events when both annihilation quanta underwent Compton scattering at $\theta_{1,2} = 90^\circ$ yielding the modulation of $R(\mu) = 2.44 \pm 0.02$ (0.418 ± 0.003). In the modified version of the setup, an active scatterer (GAGG scintillator) was placed in front of one plastic scintillator to induce decoherence by Compton scattering one of the photons before entering the polarimeter. The scattered photons then underwent another scattering in the polarimeters yielding the modulation of the azimuthal angle difference of $R(\mu) = 2.41 \pm 0.10$ (0.414 ± 0.017), a result compatible with the one obtained without intentional decoherence.

The results of Abdurashitov *et al.* [26] suggest that the correlation of the azimuthal angles of Compton scattered annihilation quanta is not affected by a prior scattering, at least at small scattering angles $\theta_{\text{scat}} \approx 0^\circ$, which disagrees with the finding of Watts *et al.* [4] suggesting the loss of correlation at $\theta_{\text{scat}} \approx 30^\circ$. The clarification of these findings is important on its own merits, but it is also relevant for the implementation of the polarization measurement in PET, where in-silico studies suggested a potential benefit of discriminating the correlated signal events from the uncorrelated background [2].

To resolve the “decoherence puzzle” arising from the previous results, we performed the most comprehensive set of measurements to date. The necessity to resolve this puzzle has also been brought up by Sharma *et al.*, [27]. Our setup based on the single-layer gamma-ray polarimeter concept [3] was able to measure the azimuthal correlation of the annihilation quanta [5, 28]. An active scatterer was placed in the path of one annihilation photon to tag the events where that gamma undergoes a prior scattering. One of the detectors could be rotated around the initial direction of the annihilation gamma, enabling the azimuthal correlation measurements at different angles of the prior Compton scattering, θ_{scat} . Thus this setup enabled recreation of the kinematic conditions similar to those in [26] ($\theta_{\text{scat}} \approx 0^\circ$) and [4] ($\theta_{\text{scat}} \approx 30^\circ$), while also significantly extending the explored phase-space to measurements with $\theta_{\text{scat}} = 10^\circ$ and $\theta_{\text{scat}} = 50^\circ$.

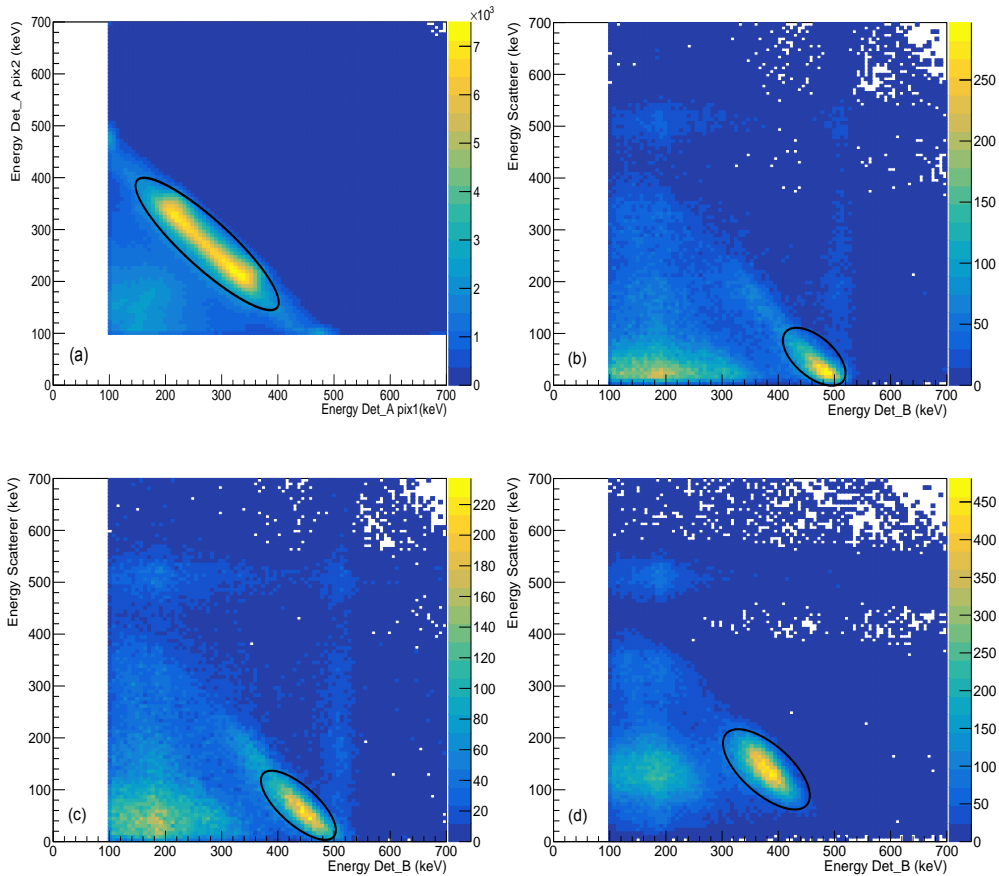


Figure 2: Energy correlation between two pixels fired in a Compton event in Detector A (a), energy correlation between Detector B and the scatterer Detector C at $\theta_{scat} = 10^\circ$ (b), at $\theta_{scat} = 30^\circ$ (c), and at $\theta_{scat} = 50^\circ$ (d). The selected events are shown with an ellipse.

2 Methodology

2.1 Experimental setup

The experimental setup consists of two single-layer gamma polarimeters [5], denoted as Detector A and B and a scatterer scintillator, denoted Detector C as shown in Figure 1. Each polarimeter encompasses 8×8 GAGG:Ce scintillator matrix with crystal dimensions $1.9 \times 1.9 \times 20 \text{ mm}^3$ and 2.2 mm pitch. The matrix is read out on one end by a silicon-photomultiplier (SiPM) array, with one-to-one match of crystals and SiPMs. The mean energy resolution (FWHM) of the GAGG:Ce detectors was $8.1 \pm 0.5\%$ at 511 keV. The scatterer (Detector C) was a single scintillating crystal of GAGG:Ce of $3.0 \times 3.0 \times 20 \text{ mm}^3$ wrapped with teflon. It was read out by one SiPM of a 8×8 SiPM array (KETEK PA3325) and its energy resolution was $12.1 \pm 0.3\%$ at 511 keV. The experiment was performed in the temperature controlled environment keeping the temperature of the Detectors A and B at $18 \pm 1^\circ\text{C}$. The temperature of the scatterer was further reduced to $15 \pm 1^\circ\text{C}$ by a Peltier-based cooling system, to improve the sensitivity for low energy events. The data were acquired using the data acquisition and processing system TOFPET2 [29, 30]. A modified set of ASIC parameters together with a lower value of time and energy thresholds were used for the data acquisition to enable the acquisition of events with low energy deposits. To do so,

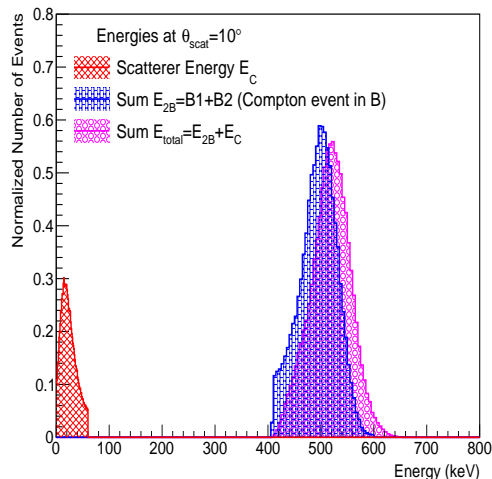


Figure 3: Energies shared among scatterer and two pixels of Detector B for $\theta_{scat} = 10^\circ$. The total sum of energies adds up to 511 keV.

the trigger threshold parameters were tuned globally to lower the baseline for dark count rejection and enable trigger for low energy events. The energy measured in each pixel was corrected for SiPM saturation and calibrated using the 511 keV photo-peak from the direct γ -rays. The calibration was independently checked with the 32 keV and 662 keV peaks of ^{137}Cs and was found to be consistent to the level of $\leq 1\%$.

In the experiment, Detector A was detecting the γ -ray coming directly from the annihilation event (denoted γ_1), while Detector B was detecting the γ_2 after scattering in the Detector C (the scatterer), which was introduced to induce decoherence by Compton scattering the annihilation photon and to tag such events. Detectors A and B were kept at a fixed distance of 5 cm from the scatterer. A ^{22}Na -source (1 mm diam., activity ≈ 370 kBq) was placed 1 cm from the scatterer between the scatterer and Detector A. The angular coverage of Detectors A and B was $\pm 10.1^\circ$ in this geometry. The events were recorded with Detector B placed at different mean scattering angles, θ_{scat} , of 0° , 10° , 30° , and 50° , while the Detector A was fixed. An additional measurement was performed to recreate the conditions of [4] with Detector B at 30° , in which the scatterer was made passive simply by switching it off, so it would not contribute to trigger or data acquisition.

2.2 Event selection

Data acquisition was triggered by coincidence events in Detector A and either of Detectors B or C ($A \cap (B \cup C)$). Further event selection was done in the analysis. To select the Compton events that occur in Detectors A or B we required the event to have a multiplicity of 2 fired pixels in the module, where a lower bound of 100 keV was applied to count a pixel as fired to avoid possible noise and cross-talk events. For Detector A, the events where two pixels fired were additionally filtered by requiring the sum of energies of the two fired pixels within 511 ± 70 keV, which corresponds to 3σ around the peak value, and to obey the Compton scattering kinematics. The resulting selection is shown by the outlined region in Figure 2 (a). To select the annihilation photons that underwent Compton scattering in Detector C and a subsequent Compton scattering following the full absorption in Detector B we required the sum of energies of two fired pixels in Detector B with Detector C are within $511 \pm 3\sigma$ keV. However different types of scattering events can satisfy this

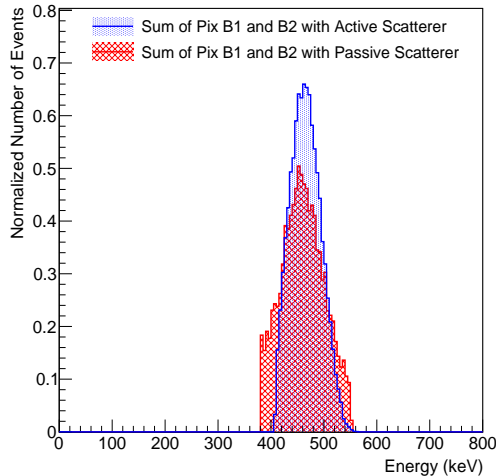


Figure 4: The sum of energies of two pixels fired in Detector B, for the selected Compton events at $\theta_{scat} = 30^\circ$, active (blue) and passive scatterer (red), using their respective selection criteria.

condition, which is why we additionally filtered those events that obey the Compton kinematics for scattering at a given θ_{scat} . The correlation of energies between Detector C and Detector B under different scattering angles (θ_{scat}) is shown in Figure 2 (b)-(d), which clearly demonstrates that the energy deposition in Detector C increases with the increasing θ_{scat} , as expected according to Compton kinematics. An example of the energy share of γ_2 in pixels selected for $\theta_{scat} = 10^\circ$ is shown in Figure 3.

A correlation-baseline measurement (without intentional decoherence), at $\theta_{scat} = 0^\circ$, was performed by selecting events where Detector C did not fire and both energy deposits in Detectors A and B were within $511 \pm 3\sigma$ keV.

An additional measurement was done with the passive scatterer, where the bias voltage of Detector C was switched off. In that case, event selection was done solely based on data from Detectors A and B. The angle of Detector B was set to $\theta_{scat}=30^\circ$ and its distance from the scatterer was increased to 7.5 cm to avoid direct coincidences between Detectors A and B. In this case, Detector B had an angular coverage of $\pm 6.8^\circ$. Although direct coincidences were avoided by the setup geometry, random coincidences of two annihilation photons from different events could contribute to the expected kinematic region. To avoid such unwanted events we additionally selected true coincidences based on their coincidence time. Hence, the events in which triggering time difference of the corresponding pixels in Detectors A and B was, $\Delta t = |t_1 - t_2| < 1.95$ ns, were selected corresponding to $\pm 3\sigma$ cut on the coincidence time peak. The energy of the selected Compton events in Detector B for $\theta_{scat}=30^\circ$ is shown in Figure 4 and is consistent with the energy spectrum of such events obtained with the active scatterer.

2.3 Determination of azimuthal correlations

For the events where both gammas underwent Compton scattering in Detectors A and B according to the conditions above, we deduce the Compton scattering angle (θ) and the azimuthal angle (ϕ) in each module as:

$$\theta = \arccos \left(\frac{m_e c^2}{E_{px1} + E_{px2}} - \frac{m_e c^2}{E_{px2}} + 1 \right); \phi = \text{atan} \left(\frac{\Delta y}{\Delta x} \right) \quad (3)$$

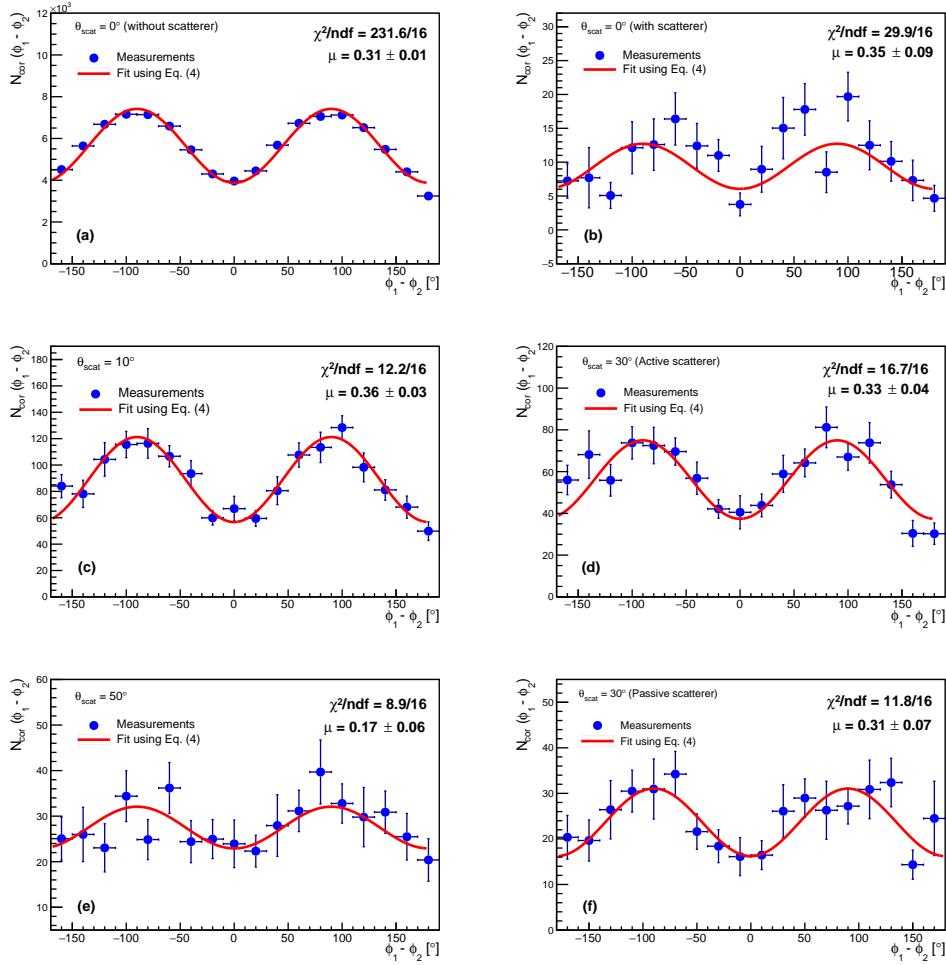


Figure 5: Azimuthal angle difference distributions for (a) direct gammas from the source, with active scatterer (b) $\theta_{\text{scat}} = 0^\circ$, (c) $\theta_{\text{scat}} = 10^\circ$, (d) $\theta_{\text{scat}} = 30^\circ$, (e) $\theta_{\text{scat}} = 50^\circ$, and (f) $\theta_{\text{scat}} = 30^\circ$ with passive scatterer, respectively. The range of Compton scattering angles, $\theta_{1,2}$, in each plot was selected to target maximum expected modulation (see section 3). Only the statistical uncertainties are shown.

Due to the ambiguity in the determination of the first and second pixels fired in Compton scattering, by the recoil electron and the scattered gamma, respectively, we have to assume that the first interaction (absorption of the recoil electron) occurs in the pixel with the lower energy deposit ($E_{\text{px1}} = E_{e'}$, $E_{\text{px2}} = E_{\gamma'}$) since the cross-section and the detector configuration favor forward scattering. According to simulations, for 511 keV gammas scattering at angles $70^\circ < \theta_{1,2} < 90^\circ$, this is true in approximately 52% of events[28]. This ambiguity does not play a significant role in determination of $\Delta\phi = \phi_1 - \phi_2$ since it is an angle between the two scattering planes. The ϕ angle is reconstructed from Δx and Δy , the distances of the fired pixel centers in the plane perpendicular to the longer crystal axis.

For the events that satisfy the Compton selection criteria and for a given range of the reconstructed angles $\theta_{1,2}$, we obtained the distribution of the azimuthal angle differences, $N(\phi_1 - \phi_2)$, where $\phi_{1,2}$ are the azimuthal angles of the Compton events in Detector A and B, respectively. The $N(\phi_1 - \phi_2)$ distributions were then corrected for detector acceptance as: $N_{\text{cor}}(\phi_1 - \phi_2) =$

$N(\phi_1 - \phi_2)/N_{\text{mixed}}(\phi_1 - \phi_2)$. The N_{mixed} is the acceptance determined by event-mixing technique [3, 5], where $(\phi_1 - \phi_2)$ is obtained by taking ϕ_1 and ϕ_2 from different randomly chosen events. For each selected Compton event in Detector A, 10^2 random uncorrelated events are sampled in Detector B.

The modulation factor, μ , is determined by fitting the acceptance-corrected distribution, $N_{\text{cor}}(\phi_1 - \phi_2)$, with

$$N_{\text{cor}}(\phi_1 - \phi_2) = M[1 - \mu \cos(2(\phi_1 - \phi_2))] \quad (4)$$

where M corresponds to the average amplitude of the distribution.

The systematic uncertainty of the determined modulation factor reflects the uncertainty in the determination of $\theta_{1,2}$ angles, resulting from the finite energy resolution of the pixels. We found this contribution to the systematic uncertainty to be 5.8% following the uncertainty of $\sigma_\theta = 6.5^\circ$. The σ_θ broadens the nominally selected $\theta_{1,2}$ window by $\theta_{1,2} \pm \sigma_{\theta_{1,2}}$ and underestimates μ around the maximum value that is achieved for $\theta_{1,2} = 82^\circ$ [5].

3 Results and discussion

The modulation of the azimuthal angle difference was measured for the annihilation quanta emerging from para-positronium detected directly and in cases where γ_2 was made decoherent following Compton scattering in the scatterer at $\theta_{\text{scat}} = 0^\circ, 10^\circ, 30^\circ$, and 50° . For quanta of 511 keV, the maximum modulation is expected for $\theta_{1,2} \approx 82^\circ$ [8, 9, 11], therefore, for $\theta_{\text{scat}} = 0^\circ$, we selected the angular range of $72^\circ < \theta_{1,2} < 90^\circ$. For scattering at $\theta_{\text{scat}} = 30^\circ$ and $\theta_{\text{scat}} = 50^\circ$ the selected angular range in detector B was $73^\circ < \theta_2 < 90^\circ$ and $74^\circ < \theta_2 < 90^\circ$, respectively. This is because the analyzing power $A(\theta) = \sin^2\theta/(\epsilon + 1/\epsilon - \sin^2\theta)$ (derived from eq. 2) [13], depends on incident gamma-ray energy, since ϵ is the ratio of scattered and incident photon energies. Therefore the maximum analyzing power for $E_2 = 450$ keV (after scattering at $\theta_{\text{scat}} = 30^\circ$) is achieved at $\theta_2 \approx 83^\circ$ and the maximum analyzing power for $E_2 = 376$ keV (after scattering at $\theta_{\text{scat}} = 50^\circ$) is achieved at $\theta_2 \approx 84^\circ$.

The acceptance-corrected distributions of the azimuthal angle differences, $N_{\text{cor}}(\phi_1 - \phi_2)$, for $\theta_{\text{scat}} = 0^\circ, 10^\circ, 30^\circ$, and 50° are shown in Figure 5. The distribution for the direct measurement (Figure 5 (a)) exhibits the expected behavior, with the maxima at $\pm 90^\circ$ indicating the initial orthogonality in the polarizations of the annihilation γ s. Similar behavior can be observed in the distributions obtained after Compton scattering by an active scatter (Figure 5 (b)-(e)) and the passive scatterer (Figure 5 (f)). The extracted modulation factors are listed in Table 1. They suggest that the strength of the modulation is largely preserved at all measured scattering angles θ_{scat} , within the precision of the experiment. Such a conclusion seems to be in line with the recent findings of Abdurashitov *et al.* [26] for $\theta_{\text{scat}} = 0^\circ$, but additionally extends the examined range up to $\theta_{\text{scat}} = 30^\circ$. Moreover, the azimuthal angle modulation is observed at $\theta_{\text{scat}} = 30^\circ$ with a passive scatterer, even though it was not evident from the measurements by Watts *et al.* [4]. We observed somewhat lower modulation for $\theta_{\text{scat}} = 50^\circ$, yielding $\mu = 0.17 \pm 0.06$, which may be a hint of a partial depolarization of γ_2 , expected for larger scattering angles [31], although this result is limited by the statistical precision.

4 Conclusions

We measured the azimuthal correlations of the gamma quanta emerging from para-positronium annihilation, based on their Compton scattering in the single-layer gamma-ray polarimeters. Mea-

Table 1: Polarimetric modulation factor, μ , for all measured configurations. The values of μ presented are subject to additional systematic underestimation of 5.8%. The data acquisition time $T_{acq.}$ in each setup is listed.

θ_{scat}°	$\mu \pm \Delta\mu_{stat.}$	$T_{acq.}(hour)$
0°	0.31 ± 0.01	48*
	$0.35 \pm 0.09^*$	
10°	0.36 ± 0.03	256
30° [†]	0.33 ± 0.04	205
30° [‡]	0.31 ± 0.07	92
50°	0.17 ± 0.06	90

*The total data acquisition duration for the direct gammas and the $\theta_{scat} = 0^\circ$ configuration. Following event selection the latter accounts for $\approx 0.15\%$ of the events. [†] $\theta_{scat} = 30^\circ$ with the active scatterer, [‡] $\theta_{scat} = 30^\circ$ with the passive scatterer

measurements were performed with one of the quanta undergoing a Compton scattering as a decohering process prior to entering the polarimeter and they are compared with the baseline measurement where the annihilation quanta are detected directly from the source. The obtained distributions of the azimuthal angle differences exhibit the modulation with maxima at $\phi_1 - \phi_2 = \pm 90^\circ$ as expected. The results show that the strength of the correlation reflected in the measured polarimetric modulation factor does not significantly differ for the case of direct quanta or the case of decoherent quanta for $\theta_{scat} = 0^\circ, 10^\circ, \text{ and } 30^\circ$. This conclusion differs from indications obtained by Watts *et al.* [4] for $\theta_{scat} \approx 30^\circ$, but it is in line with the results of Abdurashitov *et al.* [26] for $\theta_{scat} \approx 0^\circ$. For $\theta_{scat} = 50^\circ$, we observe lower modulation than at the other scattering angles investigated. Further statistically more significant measurements, especially at large scattering angles may give a more complete insight into the puzzling nature of the correlations of annihilation quanta.

Acknowledgements

This work was supported in part by the ‘‘Research Cooperability’’ Program of the Croatian Science Foundation, funded by the European Union from the European Social Fund under the Operational Programme Efficient Human Resources 2014–2020, grant number PZS-2019-02-5829, in part by QuantiXLie Center of Excellence, a project co-financed by the Croatian Government and European Union through the European Regional Development Fund — the Competitiveness and Cohesion Operational Programme, grant No. KK.01.1.1.01.0004 and in part by EU Horizon 2020 research and innovation programme under project OPSVIO, Grant Agreement No. 101038099.

Declaration of competing interest

The authors declare that they have no known competing financial interests or personal relationships that could have appeared to influence the work reported in this paper.

Data availability

Data can be made available on request.

References

- [1] A. McNamara et al., Towards optimal imaging with PET: An in silico feasibility study. *Phys. Med. Biol.*, **59**, 7587 (2014). DOI:<https://doi.org/10.1088/0031-9155/59/24/7587>
- [2] M. Toghyani et al., Polarisation-based coincidence event discrimination: An in silico study towards a feasible scheme for Compton-PET. *Phys. Med. Biol.*, **61**, 5803, (2016). DOI:<https://doi.org/10.1088/0031-9155/61/15/5803>
- [3] M. Makek et al., Single-layer Compton detectors for measurement of polarization correlations of annihilation quanta. *Nucl. Instr. Meth. Phys. Res. A*, **958**, Art. no. 162835, (2020). DOI:<https://doi.org/10.1016/j.nima.2019.162835>
- [4] D.P. Watts et al., Photon quantum entanglement in the MeV regime and its application in PET imaging. *Nat. Commun.*, **12**, 2646, (2021). DOI:<https://doi.org/10.1038/s41467-021-22907-5>
- [5] S. Parashari et al., Optimization of detector modules for measuring gamma-ray polarization in Positron Emission Tomography. *Nuclear Instrum. Methods Phys. Res. A*, **1040**, 167186, (2022). DOI:<https://doi.org/10.1016/j.nima.2022.167186>
- [6] D. Bohm, & Y. Aharonov, Discussion of experimental proof for the paradox of Einstein, Rosen, and Podolsky. *Phys. Rev.* **108**, 1070, (1957). DOI:<https://doi.org/10.1103/PhysRev.108.1070>
- [7] S.J. Bell, On the Einstein Podolsky Rosen paradox. *Physics Physique Fizika*, **1**, 195 (1964). DOI:<https://doi.org/10.1103/PhysicsPhysiqueFizika.1.195>
- [8] H.S. Snyder, S. Pasternack & J. Hornbostel, J. Angular correlation of scattered annihilation radiation. *Phys. Rev.*, **73**, 440, (1948). DOI:<https://doi.org/10.1103/PhysRev.73.440>
- [9] J.C. Ward, Some Properties of Elementary Particles, Ph.D. Thesis, University of Oxford (1949).
- [10] J. Wheeler, Polyelectrons. *Annals New York Acad. Sci.* **48**, 219, (1946). DOI:<https://doi.org/10.1111/j.1749-6632.1946.tb31764.x>
- [11] M.H.L. Pryce & J.C. Ward, Angular correlation effects with annihilation radiation. *Nature* **160**, 435, (1947). DOI:<https://doi.org/10.1038/160435a0>
- [12] O. Klein & T. Nishina, Über die Streuung von Strahlung durch freie Elektronen nach der neuen relativistischen Quantendynamik von Dirac. *Z. Phys.* **52**, 853, (1929). DOI:<http://dx.doi.org/10.1007/BF01366453>
- [13] P. Knights et al., Studying the effect of polarisation in Compton scattering in the undergraduate laboratory. *Eur. J. Phys.* **39**, 025203, (2018). DOI:<https://doi.org/10.1088/1361-6404/aa9c98>
- [14] A. Einstein, B. Podolsky, & N. Rosen, Can quantum-mechanical description of physical reality be considered complete? *Phys. Rev.* **47**, 777, (1935). DOI:<https://doi.org/10.1103/PhysRev.47.777>
- [15] A. Einstein, Zur Elektrodynamik bewegter Körper. (German) [On the electrodynamics of moving bodies]. *Ann. Phys.*, **322**, 891, (1905). DOI:<https://doi.org/10.1002/andp.19053221004>

- [16] B.C. Hiesmayr, & P. Moskal, Witnessing entanglement in Compton scattering processes via mutually unbiased bases. *Sci. Rep.* **9**, 8166, (2019). DOI:<https://doi.org/10.1038/s41598-019-44570-z>
- [17] P. Caradonna, D. Reutens, T. Takahashi, S. Takeda, V. Vegh, Probing entanglement in Compton interactions. *J. Phys. Commun.* **3**, 105005 (2019). DOI:<https://doi.org/10.1088/2399-6528/ab45db>
- [18] C.S. Wu & I. Shakhov, The angular correlation of scattered annihilation radiation. *Phys. Rev.* **77**, 136 (1950). DOI:<https://doi.org/10.1103/PhysRev.77.136>
- [19] H. Langhoff, Die linearpolarisation der vernichtungsstrahlung von positronen. *Z. Phys.* **160**, 186–193 (1960). DOI:<https://doi.org/10.1007/BF01336980>
- [20] L.R. Kasday, In *Foundations of Quantum Mechanics: Proceedings of the International School of Physics “Enrico Fermi”* (ed d’Espagnat, B.) 195–210 (Academic P XIV, 1971).
- [21] G. Faraci et al., An experimental test of the EPR paradox. *Lett. Nuovo Cim.* (1971-1985) **9**, 607–611 (1974). DOI:<https://doi.org/10.1007/BF02763124>
- [22] L.R. Kasday, J. D. Ullman & C.S. Wu, Angular correlation of Compton-scattered annihilation photons and hidden variables. *Il Nuovo Cimento B* **25** B, 633–661 (1975). DOI:<https://doi.org/10.1007/BF02724742>
- [23] A. Wilson, J. Lowe, & D. Butt, Measurement of the relative planes of polarization of annihilation quanta as a function of separation distance. *J. Phys. G: Nucl. Phys.* **2**, 613–624 (1976). DOI:<https://doi.org/10.1088/0305-4616/2/9/009>
- [24] M. Bruno, M. D’Agostino, & C. Maroni, Measurement of linear polarization of positron annihilation photons. *Il Nuovo Cimento B* **40**, 143–152 (1976). DOI:<https://doi.org/10.1007/BF02739186>
- [25] G. Bertolini, E. Diana & A. Scotti, Correlation of annihilation γ -ray polarization. *Il Nuovo Cim. B* **63**, 651–665 (1981). DOI:<https://doi.org/10.1007/BF02755105>
- [26] D. Abdurashitov et al., Setup of Compton polarimeters for measuring entangled annihilation photons, *Jour. Inst.* **17**, P03010, (2022). DOI:<https://doi.org/10.1088/1748-0221/17/03/P03010>
- [27] S. Sharma, D. Kumar, P. Moskal, Decoherence Puzzle in Measurements of Photons Originating from Electron–Positron Annihilation. *Acta Phys. Pol.*, (3) **142**, 428 (2022). DOI:<https://doi.org/10.12693/APhysPolA.142.428>
- [28] A.M. Kožuljević et al., Study of Multi-Pixel Scintillator Detector Configurations for Measuring Polarized Gamma Radiation, *Condensed Matter*, **6**, 43, (2021). DOI:<https://doi.org/10.3390/condmat6040043>
- [29] A.D. Francesco et al., TOFPET2: A high-performance ASIC for time and amplitude measurements of SiPM signals in time-of-flight applications. *J. Instr.*, **11**, Art. no. C03042, (2016).
- [30] R. Bugalho et al., Experimental characterization of the TOFPET2 ASIC. *J. Instr.*, **14**, P03029, (2019). DOI:<https://doi.org/10.1088/1748-0221/14/03/P03029>
- [31] G.O. Depaola, New Monte Carlo method for Compton and Rayleigh scattering by polarized gamma rays. *Nucl. Instr. Methods Phys. Res. A*, **512**, 619 (2013). DOI:[https://doi.org/10.1016/S0168-9002\(03\)02050-3](https://doi.org/10.1016/S0168-9002(03)02050-3)